BIOCHEMICAL PHARMACOLOGY 71 (2006) 1629–1636

available at www.sciencedirect.com

SCIENCE DIRECT®

journal homepage: www.elsevier.com/locate/biochempharm

Chemical modification at subunit 1 of rat kidney Alpha class glutathione transferase with 2,3,5,6-tetrachloro-1,4-benzoquinone: Close structural connectivity between glutathione conjugation activity and non-substrate ligand binding

Siobhan M. O'Sullivan [a,1], *Ronan M. McCarthy* [a,1], *Melissa A. Vargo* [b], *Roberta F. Colman* [b], *David Sheehan* [a,*]

[a] *Proteomics Research Group, Department of Biochemistry, University College Cork, Lee Maltings, Prospect Row, Mardyke, Cork, Ireland*

[b] *Department of Chemistry and Biochemistry, University of Delaware, Newark, DE 19716, USA*

ARTICLE INFO

Article history:
Received 24 November 2005
Accepted 3 March 2006

Keywords:
Chemical modification
Cysteine
Glutathione transferase
Alpha class
Affinity label
Structure
Tetrachlorobenzoquinone

Abbreviations:
CDNB, 1-chloro-2, 4-dinitrobenzene
DNPG, dinitrophenyl glutathione
GSH, reduced glutathione
GST, glutathione transferase
HNB, 2-hydroxyl-5-nitrobenzyl alcohol

ABSTRACT

2, 3, 5, 6-Tetrachloro-1, 4-benzoquinone (TCBQ) is a metabolite of pentachlorophenol known to react with cysteines of glutathione transferases (GSTs). TCBQ treatment of rat kidney rGSTA1-2 and rGSTA1-1 abolishes 70–80% conjugation of glutathione (GSH) to 1-chloro-2, 4-dinitrobenzene and results in strongly correlated quenching of intrinsic fluorescence of Trp-20 ($R > 0.96$). rGSTA2-2 is only inhibited by 25%. Approximately 70% (rGSTA1-1) and 60% (rGSTA1-2) conjugation activity is abolished at TCBQ: GST stoichiometries near 1:1. The inactivation follows a Kitz/Wilson model with K_D of 4.77 ± 2.5 μM for TCBQ and k_3 for inactivation of 0.036 ± 0.01 min^{-1}. A single tryptic peptide labelled with TCBQ was isolated from kidney rGSTA1-2 containing Cys-17 which we identify as the site of modification. Treatment with more than stoichiometric amounts of TCBQ modified other residues but resulted in only modest further inhibition of catalysis. We interpret these findings in terms of localised steric effects on the relatively rigid α-helix 1 adjacent to the catalytic site of subunit 1 possibly affecting the Alpha class-specific α-helix 9 which acts as a "lid" on the hydrophobic part of the active site. Homology modelling of rGSTA1-1 modified at Cys-17 of one subunit revealed only modest structural perturbations in the second subunit and tends to exclude global structural effects.

* *Corresponding author*. Tel.: +353 21 4904207; fax: +353 21 274034.
E-mail address: d.sheehan@ucc.ie (D. Sheehan).

[1] These authors contributed equally to this work.

0006-2952/$ – see front matter
doi:10.1016/j.bcp.2006.03.002

MALDI-TOF, matrix-assisted laser desorption ionisation mass spectrometry with time-of-flight detection
NEM, *N*-ethyl maleimide
TCBQ, 2,3,5,6-tetrachloro-1, 4-benzoquinone

1. Introduction

Glutathione transferases (GSTs; E.C. 2.5.1.18) comprise a complex enzyme superfamily playing a key role in Phase 2 detoxification of xenobiotics by catalysing conjugation to reduced glutathione (GSH) (for reviews, see Refs. [1,2]). Although mainly dimeric and cytosolic, a membrane-bound microsomal class also exists [3]. In addition, GSTs catalyse a variety of non-detoxification isomerisation reactions (reviewed in Ref. [1]) and possess extensive binding properties with non-substrate ligands at sites distinct from their active site [4]. Cytosolic GSTs have been classified into at least eight classes including Alpha, Mu, Pi [5], Theta [6], Sigma [7], Kappa [8], Beta [9] and Omega. [10].

In mammalian liver, both Mu and Alpha class GSTs are abundant but kidney is dominated by Alpha class enzymes [11,12]. The principal rat Alpha class subunits are denoted as 1–5, with subunit 5 forming a sub-class specialised for peroxidation reactions [2,13,14]. Subunits 1 and 2 combine to form rGSTA1-1, rGSTA2-2 and rGSTA1-2 [2]. The latter heterodimer is the most abundant GST in rat liver and kidney cytosolic extracts and is the principal component of what used to be called ''ligandin'', a GST preparation responsible for extensive ligand binding in liver cytosol [2]. Crystal structures are available for human orthologues hGSTA1-1 (Fig. 1) [15,16] and hGSTA4-4 [14] but no structure has yet been reported for GSTA2-2 or GSTA1-2 from any mammalian source. Given the 68% sequence similarity between rat subunits 1 and 2 and the fact that all GSTs studied to date follow remarkably similar folds [1], it is to be expected that the three-dimensional structure of these enzymes will resemble that of hGSTA1-1. In addition to their catalytic properties, Alpha

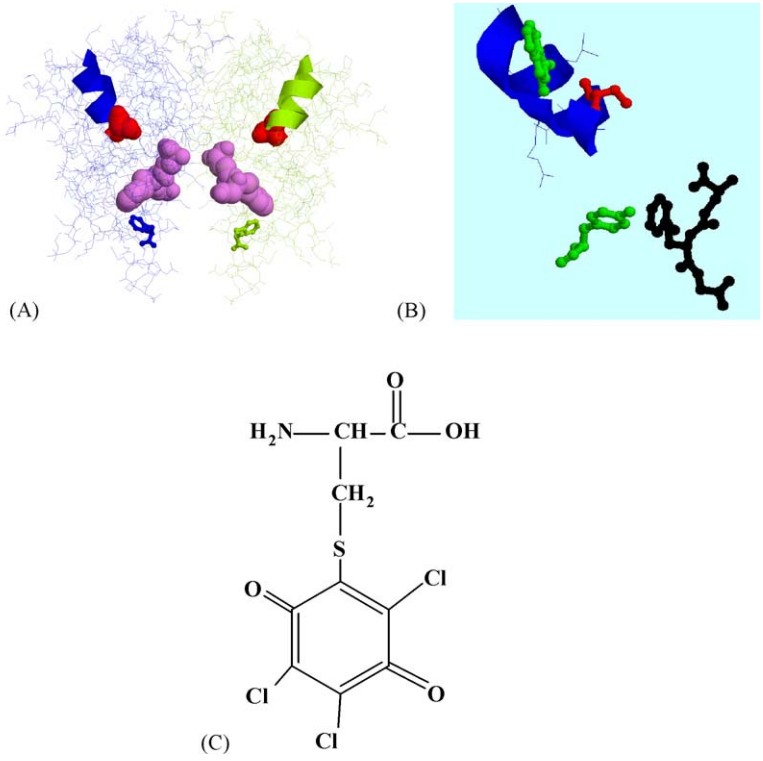

Fig. 1 – Structures of hGSTA1-1 and TCBQ. (A) Three-dimensional structure of hGSTA1-1 [15]. Subunits are presented as wireframe in green and blue, respectively. The active site is define by the ligand, *S*-bromobenzyl-GSH, presented as purple spacefill. α-Helix 1 is highlighted and the location of serine-18 (equivalent to cysteine-17 in rat subunit 1) is shown as red spacefill. Phenylalanine-222 which is part of the C-terminal α-helix 9 is presented as ball-and-stick. (B) A detail of structure of one subunit showing relative locations of tyrosine-9, *S*-benzyl-GSH and α-helix 1 with associated serine-18 and tryptophan-21. (C) Cysteine residue covalently labelled with TCBQ (for interpretation of the references to colour in this figure legend, the reader is referred to the web version of the article).

class GSTs play a key role in binding non-substrate ligands such as steroid sulphates at a single non-substrate ligand-binding site [4,17].

In all GSTs so far investigated an N-terminal loop linking the first β-sheet to the first α-helix is conserved (Fig. 1). In subunit 1 this loop and α-helix 1 are especially important in defining the part of the active site recognising the hydrophobic substrate [15,16]. By contrast, in hGSTA4-4 part of this recognition is contributed by an Alpha-class-specific C-terminal helix which is ill-defined in the apo-form of hGSTA1-1 though clearly visible in that of hGSTA4-4 and which is thought to act as a ''lid'' for the active site [14,16]. Mobility of this helix influences rate-determining steps in catalysis especially product release [18,19]. Crystallographic B factors suggest that α-helix 1 is the least flexible part of subunits 1 and 4 [14,15,19].

Site-directed mutagenesis and chemical modification have previously been used to probe the roles of cysteines in GSTs [20–22] (reviewed in Ref. [23]). Modification of Alpha class GST 2-2 by *N*-ethyl maleimide (NEM) resulted in partial inactivation but did not affect GST 1-2. 2,3,5,6-Tetrachloro-1, 4-benzoquinone (TCBQ), a metabolite of pentachlorophenol [24] and its GSH conjugate GS-1,4-TCBQ, were found to bind irreversibly at cysteines of human and rat GSTs A1-1 and A1-2 causing inhibition of catalytic activity but having little effect on GST A2-2 [23,25,26]. The GSH moiety contributes a targeting effect but does not affect the covalent labelling by the quinone moiety [25,26]. While a precise binding-site was not identified, cysteines have been suggested to be in or near the active site [27] and S-hexyl-GSH, a potent GST inhibitor, protects against GS-1, 4-TCBQ inhibition [26]. In later work, both Cys-17 and Cys-111 of rGSTA1-1 were modified by monobromobimane, an affinity label for the active site [22], while Cys-17 alone was modified by17-β-iodoacetoxy-estradiol-3-sulfate [17]. Both of these modifications produced strong inhibition of conjugation activity at the active site.

We have previously investigated non-covalent binding of a ligand, 2-hydroxy-5-nitrobenzyl alcohol (HNB), in the vicinity of the only tryptophan in subunit 1, Trp-20, and demonstrated that, while this binding strongly quenched intrinsic fluorescence at this residue, it did not inhibit catalytic activity unlike bulkier ligands which both quench fluorescence and inhibit [28]. In the present paper we identify Cys-17 in α-helix 1 of subunit 1 as the site of labelling for TCBQ. This modification is sufficient to inhibit catalytic activity by 70–80% in subunit 1 and causes closely-correlated quenching of intrinsic fluorescence although the residue is outside the active site. TCBQ is thus an additional chemical probe for α-helix 1 which offers potential for greater insight into structure–function relationships in this important GST heterodimer.

2. Materials and methods

2.1. Materials

TCBQ, 1-chloro-2, 4-dinitrobenzene (CDNB) and dinitrophenyl GSH (DNPG) were purchased from Aldrich. Trypsin (TPCK-treated), GSH and S-hexyl GSH were from Sigma. Chemicals for electrophoresis, and other analyses were of analytical grade. Adult male Wistar rats were obtained from the Biological Services Unit, University College Cork, Ireland. Chromatography resins were purchased from Whatman.

2.2. Enzyme purification

rGSTA1-1, rGSTA1-2 and rGSTA2-2 were purified from rat kidney by homogenisation in ice-cold 10 mM Tris/HCl, pH 8.0, containing 250 mM sucrose. After centrifugation (100,000 × g, 60 min), extract was dialysed against 500 ml 10 mM Tris/HCl, pH 8.0 (buffer A; 2 changes). This was applied to a DEAE-cellulose column (7 cm × 7 cm) equilibrated in buffer A. Pass-through was collected and applied to GSH-agarose (7 cm × 1.5 cm) equilibrated in buffer A containing 200 mM NaCl. Bound GSTs were eluted with 20 mM GSH in 50 mM Tris/HCl, pH 9.6, and dialysed against 10 mM sodium phosphate, pH 6.7 (buffer B; 2 changes). GSTs were applied to CM-cellulose (21 cm × 2.5 cm) equilibrated in buffer B which was developed with a 0–80 mM KCl gradient in buffer B. Purity of GSTs was assessed by SDS polyacrylamide gel electrophoresis (SDS PAGE) in 15% polyacrylamide gels [29].

2.3. Enzyme and protein assays

Conjugation activity with CDNB was assayed as previously described [30]. Protein was followed through chromatography steps by monitoring A_{280}. Protein concentrations were determined by the method of Bradford [31].

2.4. Modification with TCBQ

Purified GSTs were treated with TCBQ as previously described for Mu class enzymes [25,26]. Stock TCBQ solutions (50 μM) were prepared in ethanol and reactions performed in 100 mM potassium phosphate, pH 6.5 (25 °C). For time-dependent modification each isoenzyme (0.34 μM rGST A2-2; 1.3 μM rGST A1-2; 3 μM rGST A1-1) was incubated in a 2-fold molar excess of TCBQ. At time-intervals samples were withdrawn and immediately assayed in duplicate for CDNB conjugation activity. Extent of reaction was quantified by spectroscopically estimating the concentration of enzyme-TCBQ complex 10 min after addition of TCBQ to the enzyme. 0–0.21 μM TCBQ was added to 3 μM GST 1-1 and 1.3 μM GST 1-2 and the concentration of enzyme-TCBQ complex was determined at λ_{max} of 245 and 340 nm (residual unreacted TCBQ has a λ_{max} at 291 nm). Extinction coefficients used in these calculations were obtained from spectra collected on enzyme reacted at sub-stoichiometric TCBQ concentrations from which unreacted TCBQ had been removed by filtration in centrifugal concentrators: GST 1-1-TCBQ complex; 24,400 M^{-1} cm^{-1} (245 nM) and 11,900 M^{-1} cm^{-1} (291 nm); GST 1-2-TCBQ complex; 25,860 M^{-1} cm^{-1} (245 nM) and 12,750 M^{-1} cm^{-1} (291 nm).

2.5. Analysis of inactivation

Aliquots of enzyme (1.3 μM) were inactivated at a final TCBQ concentration of 1–8 μM. Samples were periodically removed and assayed for CDNB activity in duplicate. Rates of inactivation (k_{obs}) were determined from plots of log (% activity

remaining) versus time (min). Data were analysed by weighted non-linear regression of plots of k_{obs} versus [TCBQ] [32].

$$E + TCBQ \overset{K_D}{\rightleftarrows} E:TCBQ \xrightarrow{k_3} E-TCBQ$$

Where E represents free enzyme, E:TCBQ is a reversible complex with TCBQ and E – TCBQ is covalently labelled enzyme. k_3 is the apparent maximum achievable rate of inactivation (min^{-1}) and K_D is the apparent dissociation constant of the E:TCBQ complex. The steady state rate equation for this model is:

$$k_{obs} = \frac{k_3 \times [TCBQ]}{K_D + [TCBQ]}$$

Inactivation studies in the presence of inhibitors S-hexyl-GSH and dinitrophenyl-GSH (DNP-GSH) were performed as above but with pre-incubation of enzyme with 100 μM inhibitor (10 min).

2.6. Fluorescence measurements

Tryptophan fluorescence was determined (SLM Aminco Bowman 8000C spectrofluorimeter) by exciting at 300 nm and measuring emission in the range 300–540 nm. Protein (3 μM) was placed in a 1 ml quartz cuvette in 10 mM sodium phosphate, pH 7.0, and 0–8 μM TCBQ was added in stepwise additions at 25 °C. Spectra were recorded on each sample until no further change was observed (usually within 2 min). Measurements made at an emission wavelength of 334 nm were used to follow quenching of intrinsic fluorescence due to tryptophan-20.

2.7. Isolation and analysis of TCBQ-labelled peptide

Kidney rGSTA1-2 (100 μg) treated with a stoichiometric amount of TCBQ for 20 min was concentrated to approx 10 μl in a centrifugal concentrator, diluted to 500 μl and reconcentrated twice to remove unreacted TCBQ. The enzyme was then digested with 1 μg TPCK-treated trypsin (25 °C overnight). Peptides were applied to a Sep-Pak™ (reversed phase C-18) cartridge pre-equilibrated by washing successively in 100% acetonitrile, 0.1% trifluoroacetic acid (TFA) and aqueous 0.1% TFA. Peptides were eluted by washing successively with increasing 2% acetonitrile aliquots in 0.1% TFA. Samples of each fraction were analysed for A_{210} and A_{340} (λ_{max} of Cys-TCBQ complex) [25]. A single fraction giving a high A_{340} was diluted 1:1 with aqueous 0.1% TFA and re-applied to a second Sep-Pak™ cartridge. Peptides were re-eluted with 1% increasing acetonitrile concentration steps. Purity of peptides was determined by reversed phase C-18 HPLC. TCBQ-labelled peptide was analysed by matrix-assisted laser desorption ionisation mass spectrometry with time-of-flight detection (MALDI-TOF MS) at the Proteome Facility, University of Aberdeen, Scotland UK.

2.8. Protein graphics

Representations of hGSTA1-1 were generated with the programme RasTop version 2.0.3. [33] using the PDB file (1GUH) for hGSTA1-1 [15]. Serine-18 of hGSTA1-1 corresponds to rGSTA1-1 cysteine-17. A model of rGSTA1-1 was created with the homology modelling facility of Insight II run on a Silicon Graphics machine [17]. The PDB file (1GUH) was downloaded from the Protein Database and the co-crystallised ligand S-benzyl GSH was removed. Individual residues were changed to create the sequence of rat subunit 1. TCBQ was attached covalently at cysteine-17 and several iterations of energy minimisation were gone through to generate a model for a TCBQ-labelled rGSTA1-1.

3. Results

3.1. TCBQ labelling Inhibits GST activity

TCBQ modification (Fig. 2) causes rapid inhibition of conjugation activity which is more pronounced in rGSTA1-1 and rGSTA1-2 than rGSTA2-2. Inactivation kinetics of rGSTA1-2 obey a Kitz and Wilson model [34] (inset to Fig. 2) with $k_3 = 0.036 \pm 0.01\ min^{-1}$ and $K_D = 4.77 \pm 2.5$ μM. These data suggest high affinity for TCBQ and rapid inactivation.

Cysteines are the major targets for TCBQ in GSTs and the number of cysteines modified in rGSTA1-1 and rGSTA1-2 may be estimated spectrophotometrically [25,27]. Modification of a single cysteine accounted for most inhibition of catalytic activity for rGSTA1-1 and rGSTA1-2 (60% and 80%, respectively) while modification of a further two cysteines resulted in abolition of >85% activity (Fig. 3). At identical GST dimer concentrations, rGSTA1-2 appeared to be more sensitive to TCBQ modification than rGSTA1-1 (Figs. 2 and 3). However, when assayed at uniform TCBQ: subunit 1 ratios, similar levels of inhibition were found after a 3-min incubation (40% and 37%, respectively for rGSTA1-1 and rGSTA1-2). At near-maximum inhibition of rGSTA1-1 catalysis (~80%), approximately seven TCBQ molecules bound per GST dimer (Fig. 3). At 80% inhibition of rGSTA1-2, approximately 3 TCBQ molecules bound per dimer. These data suggest that subunit 1 is targeted

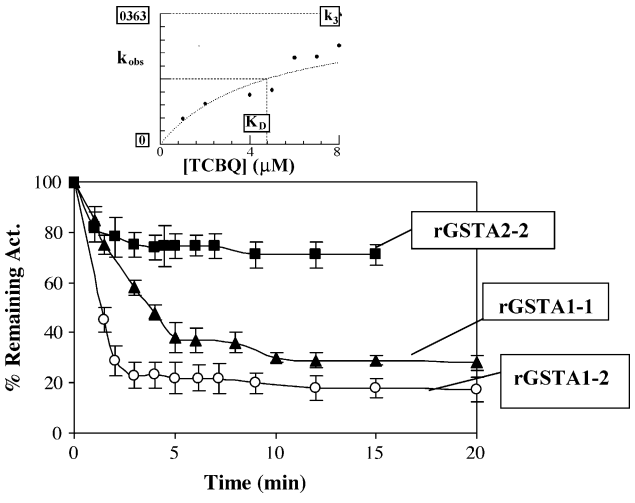

Fig. 2 – Time course for inactivation of Alpha class GSTs by TCBQ. Aliquots of purified GSTs were treated with TCBQ as described in Section 2 and conjugation activity with CDNB measured for 15–20 min. Inset, Non-linear regression analysis of inactivation of rGSTA1-2.

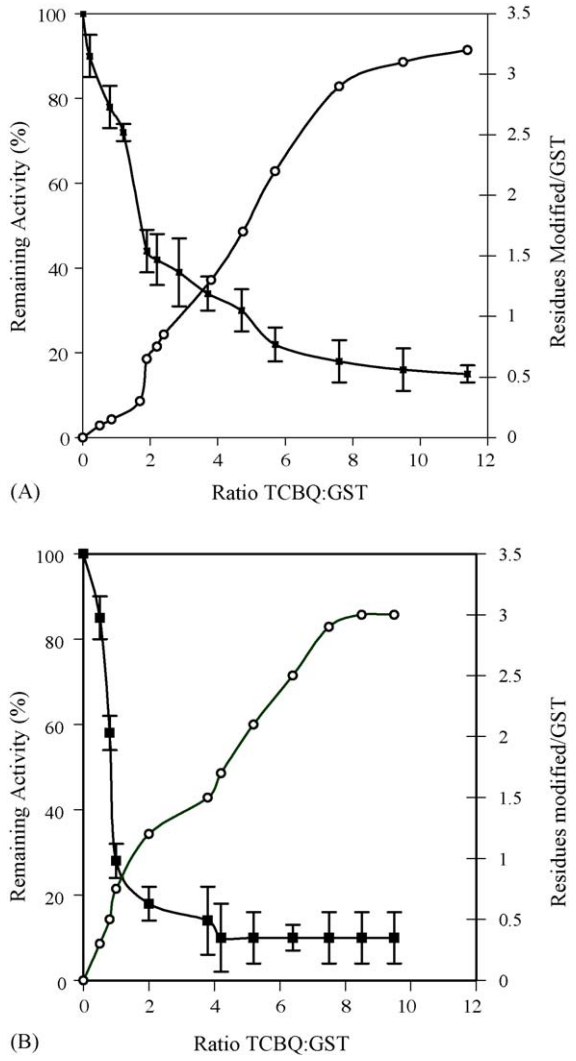

Fig. 3 – Labelling of cysteines with TCBQ. Number of cysteines labelled (open circles) was determined spectrophotometrically as described in Section 2. Residual catalytic activity with CDNB is shown as filled circles. (A) rGSTA1-1. (B) rGSTA1-2.

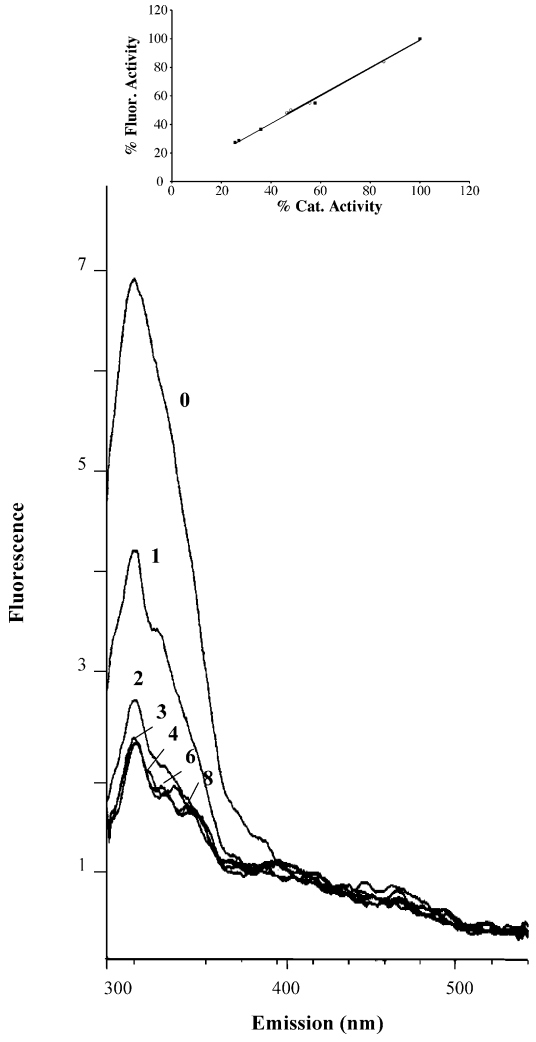

Fig. 4 – Fluorescence spectra of rGST A1-2 treated with TCBQ. Excitation wavelength was 300 nm and emission was measured in the range 300–540 nm. Spectra are shown for untreated enzyme (0) and enzyme treated with 1–8 mM TCBQ. Inset: correlation between fluorescence quenching and inhibition of catalytic activity for rGST A1-1 (filled squares) and rGSTA1-2 (open circle).

by TCBQ in both rGSTA1-1 and rGSTA1-2. Despite 68% sequence identity with subunit 2, subunit 1 reacts preferentially with TCBQ leading to strong inhibition of catalytic activity due to modification of a single cysteine.

3.2. *TCBQ labelling quenches intrinsic fluorescence associated with tryptophan-20 which is highly correlated with inhibition of catalysis*

Tryptophan-20 is the strongest intrinsic fluor in subunit 1 and ligand binding frequently quenches this fluorescence. TCBQ modification of rGSTA1-1 and rGSTA1-2 caused strong quenching of tryptophan-20 fluorescence (Fig. 4). The strong correlation between fluorescence quenching and inhibition of catalytic activity ($R > 0.96$ for both isoenzymes; inset to Fig. 4) suggests that structural perturbations resulting from TCBQ labelling underlie both processes. α-Helix-1 is the least flexible part of subunit 1 which may explain why ligands binding at this helix can ''transmit'' effects so readily into the active site [15,18,19,28].

3.3. *TCBQ modifies at a site adjacent to but outside the catalytic site*

Notwithstanding strong effects on both catalytic activity and intrinsic fluorescence associated with TCBQ modification, the product analogue DNPG and inhibitor S-hexyl-GSH only partially protected against TCBQ modification (Fig. 5) while GSH alone resulted in even more modest protection (not shown). The site of TCBQ binding is not therefore within the active site but is adjacent to it. The GSH-TCBQ conjugate strongly protects Alpha class GSTs from inactivation which underlines the ''targeting'' effect of the GSH moiety of this compound [25].

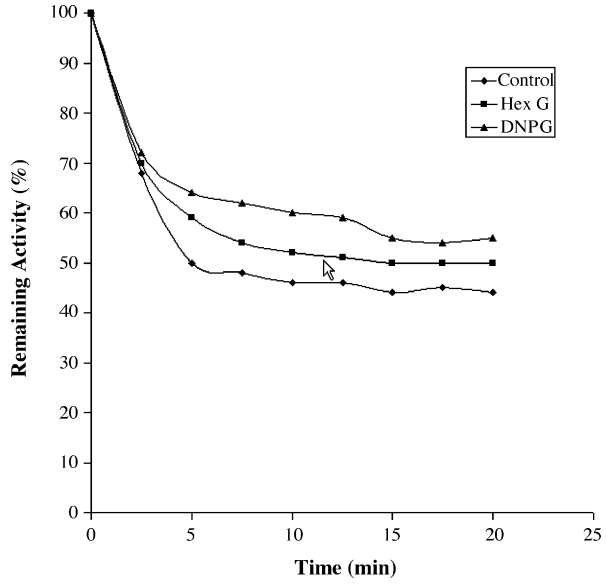

Fig. 5 – Protection of rGSTA1-2 against inactivation by TCBQ. Enzyme (1.3 μM) was pre-incubated with 100 μM DNPG (filled triangles) or *S*-hexyl-GSH (filled boxes) and modified with TCBQ as described in Section 2. Results are expressed relative to untreated enzyme (open circles).

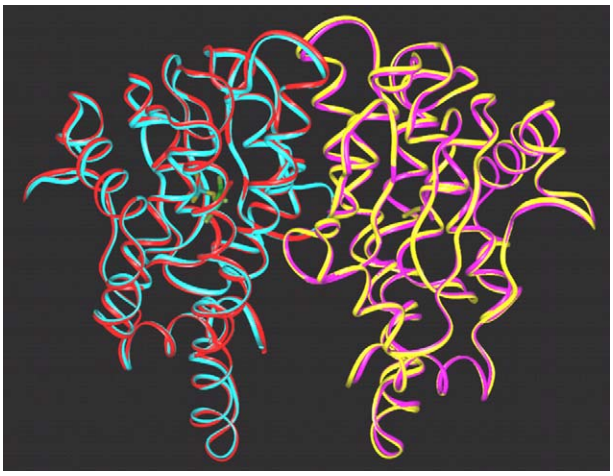

Fig. 7 – Homology model of rGST A1-1. Models for enzyme complexed with (red and yellow) and without (cyan and pink) TCBQ are shown. The TCBQ moiety is shown as a ball-and-stick structure attached to cysteine-17 of the left-hand subunit. Note the small extent of structural perturbation introduced by TCBQ modification (for interpretation of the references to colour in this figure legend, the reader is referred to the web version of the article).

3.4. *TCBQ labels cysteine-17 specifically*

A single peptide was identified in tryptic digests of TCBQ-labelled kidney rGSTA1-2 by a strong A_{340}/A_{210}. The peptide was isolated by preparative reverse phase chromatography (Fig. 6). This preparation gave a single peak on C-18 reverse phase HPLC (not shown) and MALDI-TOF analysis yielded major *m*/*z* peak values of 876.39 and 892.36, respectively, with two smaller peaks of *m*/*z* 860.43 and 908.32. A peptide comprising residues 15–19 (NH_2-Met-Glu-Cys-Ile-Arg–COOH) when labelled with TCBQ would have a predicted *m*/*z* of 859.26 which is in reasonable agreement with the experimental value of 860.43 under the measurement conditions used. Peak values of approx. +16 (*m*/*z* 876.39) and +32 (*m*/*z* 892.36) are consistent with a peptide containing methionine–sulphoxide and methionine–sulphone, respectively. No special precautions were taken to protect the peptide from oxidation during isolation and residues 15–19 include methionine-15. The three main MS peaks comprise a fingerprint for a TCBQ-labelled tryptic peptide corresponding to residues 15–19 plus two oxidation products. We attribute minor peaks of 854.43 and 908.32 to trace contaminants of the peptide. From this we conclude that cysteine-17 is the site at which TCBQ preferentially reacts.

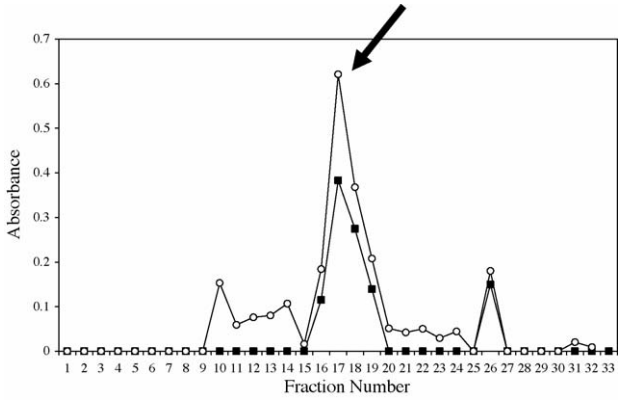

Fig. 6 – Preparative reversed phase C-18 chromatography of tryptic digest of rGSTA1-2. A single peptide showing strong absorbance at both 210 and 340 nM is shown (arrow). This was collected and analysed by mass spectrometry.

3.5. *Homology modelling suggests TCBQ exerts localised effects*

Binding stoichiometries near 1 for rGSTA1-1 suggest the possibility that TCBQ labelling of one subunit may preclude labelling at the corresponding site of the other subunit. In order to address this we created a homology model for rGSTA1-1 and then included a TCBQ label at cysteine-17 of one subunit (Fig. 7). Only very modest structural effects on the unlabelled subunit were visible in this model. Interestingly, such effects as were visible were concentrated on the C-terminal α-Helix-9 which forms a "lid" for the active site of the other subunit [18,19]. This may explain inhibition of catalysis on the unlabelled subunit but it remains unclear why only one cysteine-17 is labelled per dimer. This model suggests that TCBQ modification exerts localised rather than global structural effects on GSTs which implies that it may be an especially useful probe for investigating structure–function relationships between the processes of catalysis and non-substrate ligand binding.

4. Discussion

Alpha class enzymes are the most abundant GSTs in mammalian liver and have relatively low k_{cat}/K_m ratios. This, coupled with their extensive binding properties, suggests that ligand binding may be a more important in vivo role for these proteins than catalysis. Understanding structure–function linkages between ligand binding and catalysis is therefore especially important in this family of detoxification enzymes. Quenching of intrinsic fluorescence due to tryptophan-20 is widely used as a probe for ligand binding and the crystal structure of hGSTA1-1 explains this in terms of the proximity of α-helix 1 to the active site as defined by the co-crystallised ligand *S*-benzyl GSH (Fig. 1; [15]).

Either alone, or in the form of its GSH conjugate TCBQ has been demonstrated to inactivate rat Alpha and Mu class GSTs irreversibly by binding at a single cysteine on each subunit under conditions of 5-fold molar excess of TCBQ to subunit [25]. The observed stoichiometry of labelling was 1:1 for TCBQ:GST subunit [26]. However these investigations did not identify a specific site of attachment of TCBQ and preceded the availability of crystal structures which limited interpretation of structure–function effects. In the present study, we have carried out generally similar experiments but at a significantly lower TCBQ molar excess. We observed that it was possible to abolish 80% (rGSTA1-2) and 70% (rGSTA1-1) of conjugation activity by treatment of enzyme in as little as 2-fold molar excess of TCBQ to GST subunit in a 5-min time-frame which compares to corresponding values of 89% and 93% reported previously [25]. At this lower stoichiometry, a single cysteine was found to be labelled in each dimer rather than one per subunit [25,26]. This suggests that our conditions represent an earlier stage of saturation of these proteins with TCBQ. Quenching of intrinsic fluorescence due to tryptophan-20 correlates strongly with inhibition of catalytic activity ($R > 0.96$) suggesting that the site of labelling is on or very near α-helix-1 (Fig. 1). It is known that ligand binding at this helix causes quenching of fluorescence and that the helix is especially rigid and thus may transmit structural changes into the nearby active site. We previously showed that a small ligand, HNB, was capable of quenching fluorescence without causing inhibition of catalytic activity while larger ligands caused both quenching and inhibition [28]. The site of TCBQ labelling seems to be outside the active site as both DNPG and *S*-hexyl-GSH confer only partial protection against inactivation. Previous observations showed that inactivation caused by the GSH-TCBQ conjugate is strongly inhibited by *S*-hexyl-GSH [25]. It is possible that this may reflect differences in the hydrophobic part of the active-site or differences between TCBQ and its GSH conjugate. It is known that the latter molecule is a more potent inhibitor than unconjugated TCBQ [25]. The lack of DNPG protection suggests that the site of modification is outside the active site proper and therefore labelling with TCBQ causes inhibition by a structural perturbation transmitted into the active site.

Analysis of an isolated TCBQ-labelled peptide from part of α-helix-1 identified cysteine-17 as the labelled residue. Modification at this residue explains strong quenching of tryptophan-20 intrinsic fluorescence by TCBQ modification since it is very near cysteine-17. Moreover, binding of a bulky substituent to this most rigid helix in subunit 1 would be expected to cause an effect on the nearby active site: the loop linking this helix to β-1 contains active site residues. The >50% inhibition observed in both rGSTA1-1 and rGSTA1-2 under conditions where a single residue is modified suggests that covalent modification at cysteine-17 of one subunit may cause structural perturbation on the other subunit. Modification of methionine-208 of one subunit of Alpha class GST by the photoaffinity label glutathionyl *S*-(4-(succinimidyl)benzophenone) abolished enzyme activity of both subunits [35]. It has also been shown that covalent labelling at cysteine-17 of one subunit of rGSTA1-1 by 17 β-iodoacetoxy-estradiol-3-sulphate precluded labelling by this compound at cysteine-17 of the second subunit [17]. Construction of a homology model of modified GST showed that the estradiol sulphate affinity label sterically occluded access to the corresponding site on the second subunit [17]. In the present work, a similar homology model for TCBQ-labelled rGSTA1-1 was constructed. This revealed only modest structural changes as a result of TCBQ labelling such as slight alterations in a C-terminal portion of the unlabelled subunit containing α-helix 9. This helix is a class-specific structural feature acting as a ''lid'' for the catalytic site which plays an active part in catalysis [18,19] We cannot exclude the possibility that labelling of cysteine-17 of one subunit may affect an amino acid at the subunit interface, which in turn subtly influences the structure and activity of the second subunit. Arginine-69 is a critical subunit interface participant [36] and TCBQ is only about 3.5 Å from this residue in the same subunit. This structural perturbation, though modest, may be large enough to affect the unlabelled subunit thus causing inhibition at the second active site. In any event, the model suggests that effects of TCBQ on GST structure are most likely to be local rather than global. Thus, TCBQ provides a potential chemical probe for a region adjacent both to the active site and to tryptophan-20, a key reporter molecule for non-substrate ligand binding.

REFERENCES

[1] Sheehan D, Meade G, Foley VM, Dowd C. Structure, function and evolution of glutathione transferases: implications for classification of non-mammalian members of an ancient enzyme superfamily. Biochem J 2001;360:1–16.
[2] Hayes JD, Flanagan JU, Jowsey IR. Glutathione transferases. Ann Rev Pharmacol Toxicol 2005;45:51–88.
[3] Jakobsson PJ, Morgenstern R, Mancini J, Ford-Hutchinson A, Persson B. Common structural features of MAPEG–a widespread superfamily of membrane-associated proteins with highly divergent functions in eicosanoid and glutathione metabolism. Protein Sci 1999;8:689–92.
[4] Listowsky I, Abramowitz M, Hanuna H, Nitu Y. Intracellular binding and transport of hormones and xenobiotics by glutathione *S*-transferase. Drug Metab Rev 1988;19:305–18.
[5] Mannervik B, Alin P, Guthenberg C, Jensson H, Tahir MK, Warholm M, et al. Identification of three classes of cytosolic glutathione transferases common to several mammalian species: correlation between structural data and enzymatic properties. Proc Natl Acad Sci USA 1985;82:7202–6.
[6] Meyer DJ, Coles B, Pemble SE, Gilmore KS, Fraser GM, Ketterer B. Theta, a novel class of glutathione

S-transferases purified from rat and man. Biochem J 1991;274:409–14.
[7] Buetler TM, Eaton DL. Glutathione S-transferases–amino acid sequence comparison, classification and phylogenetic relationship. Environ Carcinogen Ecotoxicol Rev 1992;C10:181–203.
[8] Pemble SE, Wardle AF, Taylor JB. Glutathione S-transferase class Kappa: characterization by the cloning of mitochondrial GST and identification of a human homologue. Biochem J 1996;319:749–54.
[9] Rossjohn J, Polekhina G, Feil SC, Allocati N, Masulli M, Di Ilio C, et al. A mixed disulfide bond in bacterial glutathione transferase: functional and evolutionary implications. Structure 1998;6:721–34.
[10] Board PG, Coggan M, Chelvanayagam G, Eastal S, Jermin LS, Schulte GK, et al. Identification, characterization and crystal structure of the Omega class glutathione transferases. J Biol Chem 2000;275:24798–806.
[11] Scully NC, Mantle TJ. Tissue distribution and subunit structures of the multiple forms of glutathione S-transferase in the rat. Biochem J 1981;193:367–70.
[12] Rowe JD, Nieves E, Listowsky I. Subunit diversity and tissue distribution of human glutathione S-transferases: interpretations based on electrospray ionisation-MS and peptide sequence-specific antisera. Biochem J 1997;325:481–6.
[13] Hubatsch I, Ridderstrom M, Mannervik B. Human glutathione transferase A4-4: an Alpha class enzyme with high catalytic efficiency in the conjugation of 4-hydroxynonenal and other genotoxic products of lipid peroxidation. Biochem J 1998;330:175–9.
[14] Bruns CM, Hubatsch I, Ridderstrom M, Mannervik B, Tainer JA. Human glutathione transferase A4-4 crystal structures and mutagenesis reveal the basis of high catalytic efficiency with toxic lipid peroxidation products. J Mol Biol 1999;288:427–39.
[15] Sinning I, Kleywegt GJ, Cowan SW, Reinemer P, Dirr HW, Huber R, et al. Structure determination and refinement of human alpha class glutathione S-transferase A1-1, and a comparison with the mu and pi class enzymes. J Mol Biol 1993;232:192–212.
[16] Cameron AD, Sinning I, L'Hermite G, Olin B, Board PG, Mannervik B, et al. Structural analysis of human Alpha–class glutathione transferase A1-1 in the apo-form and in complex with ethacrynic acid and its glutathione conjugate. Structure 1995;3:717–27.
[17] Vargo MA, Colman RF. Affinity labelling of rat glutathione S-transferase isozyme 1-1 by 17-beta-iodoacetoxy-estradiol-3-sulphate. J Biol Chem 2001;276:2031–6.
[18] Nilsson LO, Edalat M, Pettersson PL, Mannervik B. Aromatic residues in the C-terminal region of glutathione transferase A1-1 influence rate-determining steps in the catalytic mechanism. Biochim Biophys Acta 2002;1598:157–63.
[19] Kuhnert DC, Sayed Y, Mosebi S, Sayed SM, Sewel Tl, Dirr HW. Tertiary interactions stabilise the C-terminal region of human glutathione transferase A1-1: a crystallographic and calorimetric Study. J Mol Biol 2005;349:825–38.
[20] Chang LH, Wang LY, Tam MF. The single cysteine residue on an Alpha family chick liver glutathione S-transferase CL 3-3 is not functionally important. Biochem Biophys Res Commun 1991;180:323–8.
[21] Nishihira J, Ishibashi T, Sakai M, Nishi S, Kumazaki T, Hatanaka Y, et al. Characterization of cysteine residues of glutathione S-transferase P—Evidence for steric hindrance of substrate binding by a bulky adduct to cysteine-47. Biochem Biophys Res Commun 1992;188:424–32.
[22] Hu LQ, Colman RF. Resonance energy transfer between sites in rat liver glutathione S-transferase, 1-1, selectively modified at cysteine-17 and cysteine-111. Biochemistry 1997;36:1635–45.
[23] van der Aar EM, Tan KT, Commandeur JNM, Vermeulen NPE. Strategies to characterize the mechanisms of action and the active sites of glutathione S-transferases: a review. Drug Metab Rev 1998;30:569–643.
[24] van Ommen B, Adang A, Müller F, van Bladeren PJ. The microsomal metabolism of pentachlorophenol and its covalent binding to protein and DNA. Chem-Biol Interactions 1986;60:1–11.
[25] van Ommen B, den Besten C, Rutten ALM, Ploemen JHTM, Vos RME, Müller F, et al. Active site-directed irreversible inhibition of glutathione S-transferases by the glutathione conjugate of tetrachloro-1,4-benzoquinone. J Biol Chem 1988;263:12939–42.
[26] Ploemen JHTM, van Ommen B, van Bladeren PJ. Irreversible inhibition of human glutathione S-transferase isoenzymes by tetrachloro-1,4-benzoquinone and its glutathione conjugate. Biochem Pharmacol 1991;41:1665–9.
[27] Carne C, Tipping E, Ketterer B. The binding and catalytic activities of forms of ligandin after modification of its thiol groups. Biochem J 1979;177:433–9.
[28] McCarthy R, Farmer P, Sheehan D. Binding of 2-hydroxy-5-nitrobenzyl alcohol to rat alpha class glutathione S-transferases: evidence for binding at tryptophan-21. Biochim Biophys Acta 1997;1293:185–90.
[29] Laemmli UK. Cleavage of structural proteins during the assembly of the head of bacteriophage T4. Nature 1970;227:680–5.
[30] Habig WH, Pabst MJ, Jakoby WB. Glutathione S-transferases: the first step in mercapturic acid formation. J Biol Chem 1974;249:7130–9.
[31] Bradford MM. A rapid and sensitive method for the quantitation of microgram quantities of protein using the principle of protein-dye binding. Anal Biochem 1976;72:248–54.
[32] Cleland WW. Statistical analysis of enzyme kinetic data. Methods Enzymol 1979;63:103–38.
[33] Valladon P. http://www.geneinfinity.org/rastop/; 2000.
[34] Kitz R, Wilson IB. Esters of methanesulfonic acid as irreversible inhibitors of acetylcholinesterase. J Biol Chem 1962;237:3245–9.
[35] Wang J, Baumann S, Colman RF. Probing subunit interactions in alpha class rat liver glutathione S-transferase with the photoaffinity label glutathionyl S-[4-(succinimidyl)benzophenone]. J Biol Chem 2000;275:5493–503.
[36] Vargo MA, Nguyen L, Colman RF. Subunit interface residues of glutathione S-transferase A1-1 that are important in the monomer–dimer equilibrium. Biochemistry 2004;43:3327–35.